ISTITUTO NAZIONALE DI FISICA NUCLEARE

Laboratori Nazionali di Frascati

SPARC/EBD-07/003

23 Luglio 2007

Accurate emittance calculation from phase space analysis

A. Cianchi[1], C. Ronsivalle[2], L. Giannessi[2], M. Quattromini[2],
M. Castellano[3], D. Filippetto[3]

[1)] *INFN, Sezione di Roma Tor Vergata, I-00173 Roma, Italy*

[2)] *ENEA, Via E. Fermi, 00044 Frascati, Roma, Italy*

[3)] *INFN, Laboratori Nazionali di Frascati, P.O. Box 13, I-00044 Frascati, Italy*

Abstract

The SPARC emittance meter opened new possibility in the study of beam dynamics, allowing measurements of the beam parameters evolution downstream the RF gun. Due to the used technique and the large number of the samples a precise reconstruction of the transverse phase space was also obtained. In addition to being a visual aid in understanding the beam dynamics, the phase space contains valuable information. We developed this new algorithm to extract the emittance value directly from the phase space data.

PACS:11.30.Er,13.20.Eb;13.20Jf;29.40.Gx;29.40.Vj

Published by **SIS-Pubblicazioni**
Laboratori Nazionali di Frascati

1 Introduction

The SPARC emittance meter [1] allowing emittance measurements in different z position (being z the longitudinal distance from the cathode) has given a complete reconstruction of the electron beam dynamics in the region downstream of the RF Gun where the emittance compensation process acts. The conventional algorithm [2] developed to retrieve the emittance value must firstly define the separation between the signal and the noise, including in this also the beam halo. Several thresholds are needed to isolate the beam contribution. In this operation a certain, and undefined, percentage of the beam is cut away. To allow comparison with different algorithms and method it is needed to quantify this level. Moreover, finding a clear marker for the separation between the beam and the halo is interesting to define a standard reference point.

The technique of measuring the beam emittance and the phase space, in both the horizontal and vertical planes, makes use of a double system of horizontal and vertical slit masks [3]. Selecting an array of beamlets by means of an intercepting multi-slit mask, alternatively creating one beamlet using a single slit moving transverse over the beam spot, reduces the space charge dominated incoming beam into emittance-dominated beamlets that drift up to an intercepting screen. If the screen response is linear, the intensity of beamlets spots on the screen are directly proportional to the number of particles in the beamlets which hit the screen. The emittance can be retrieved calculating the second momentum of the beam distribution as reported in [4]. The procedure to generate the transverse phase space from the beam images is discussed widely in [2]. An example of the results is shown in the Fig. 1.

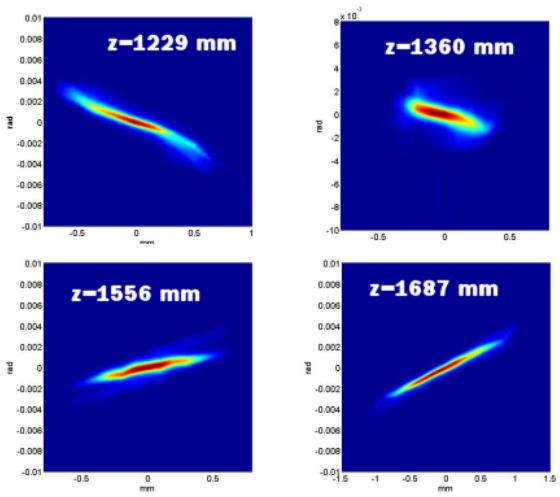

Figure 1: Phase space reconstructed for measurements in different z positions

The goal of this work is to find a unambiguous method to calculate the emittance value starting from these pictures, giving an estimation of the cut operated on the beam by the traditional algorithm [2]. The basic idea is to associate to every pixel of the image its contribution to the total emittance. Sorting them using the emittance as order parameter is possible to cut away those which have highest contribution on the emittance value. A phenomenological evidence, coming from the analysis of our data, shows that the second derivative of the emittance versus charge has a sharp, clear peak. Simulation with Monte-carlo routine demonstrated that this point is associated to the transition between the signal and the noise, in certain conditions.

2 Raw phase space

The starting phase space coming from already cited algorithm is produced with just a crude background subtraction. In Fig. 2 is possible to appreciate the very high SNR (signal to noise ratio) of the phase space beam signal respect to the residual background. It is shown a real phase space, where the intensity was expanded in the vertical direction.

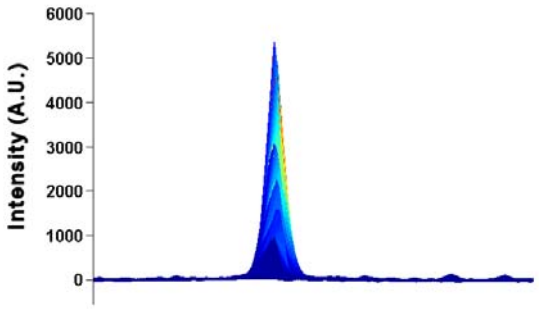

Figure 2: SNR of typical initial phase space

Some noise is still present. The flow chart of this section of the algorithm is described in Fig 3. The first operation is the selection of a region of interest in the 2D phase space around the beam area. Only the pixel inside this area will be used for the calculation. In this way it is possible to largely reduce the computing time. The background subtraction routine that is used to produce the phase spaces leaves some negative values in the data, due to the fact that the noise has an oscillating value. The program recognizes the negative values and starting from the first found on every side closest to the beam, mark them with different color as it can be seen in Fig. 4.

From this figure is possible to appreciate the structure of the 13 original profiles that were used to produce the interpolated phase space. All the pixels farer from the

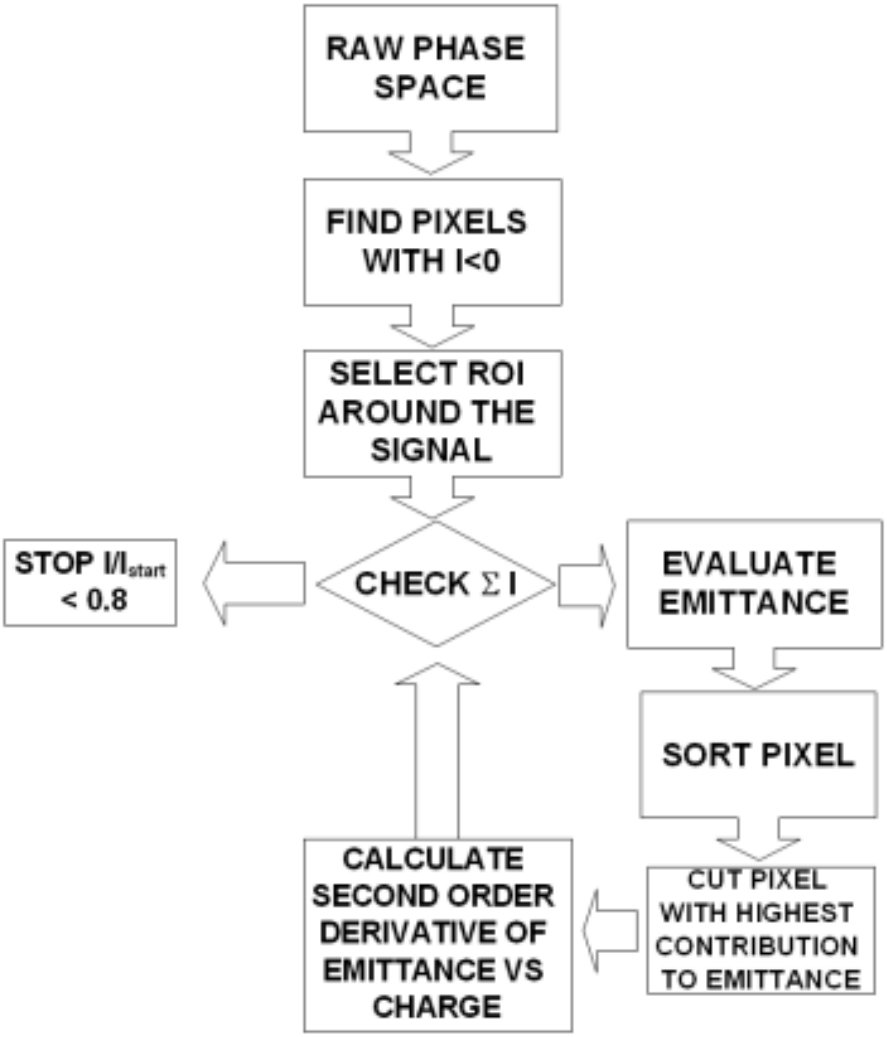

Figure 3: flow chart

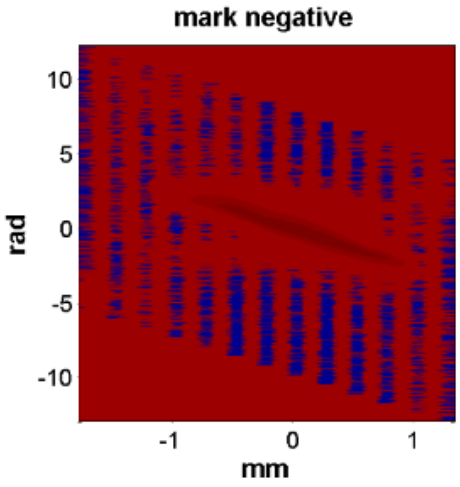

Figure 4: Negative values marked

signal more than the first negative value are set to zero. Again from Fig. 4 is possible to appreciate that no part of the signal is cut in this way. This is reasonable because if there is a pixel with negative value it means that, on average, the value of this pixel is below the mean background. And this is more valid for others that are farer from the signal respect to this one.

From the coordinates and the intensity of every pixel all the values x_i,y_i,I_i, being x the position, y the vertical coordinate (i.e. the angular divergence) and I the intensity of the i-th pixel, are retrieved . These data are used for a first evaluation of the emittance based on the calculation of the second order momentum of the distribution. To simplify the calculation the average values are evaluated and subtracted, so that $\langle\overline{x}\rangle$=0 and $\left\langle\overline{x'}\right\rangle$=0 The second order momentum are so calculated:

$$\left\langle\overline{x^2}\right\rangle = \frac{1}{\sum I_i}\sqrt{\sum I_i x_i^2} \tag{1}$$

$$\left\langle\overline{x'^2}\right\rangle = \frac{1}{\sum I_i}\sqrt{\sum I_i x_i'^2} \tag{2}$$

$$\langle\overline{xx}\rangle = \frac{1}{\sum I_i}\sqrt{\sum I_i x_i x_i'} \tag{3}$$

It's important to mention that the summation index *i* is the pixel number ranging from 1 to the total number of the pixels. The geometrical emittance is then retrieved by

$$\epsilon = \sqrt{\left\langle\overline{x^2}\right\rangle\left\langle\overline{x'^2}\right\rangle - \langle\overline{xx}\rangle^2} \tag{4}$$

Using the Courant-Snyder invariant

$$\epsilon_i = \gamma x_i^2 + 2\alpha x_i x_i' + \beta x_i'^2 \tag{5}$$

is possible to associate at each pixel its contribution to the total emittance. The program generates so a table(Tab. 1) with on the column the pixel number, its horizontal position, its vertical position, its intensity and its contribution to the total emittance.

Pixel #	Position x	Position y	Intensity	Emittance
i	x_i	y_i	I_i	ϵ_i
i+1	x_{i+1}	y_{i+1}	I_{i+1}	ϵ_{i+1}
.	.	.	.	.
.	.	.	.	.

Table 1: Table built with the data

All the pixel are sorted using their contribution to the emittance as order parameter. Starting with the one with highest contribution to the emittance the pixel are cut one by one calculating every time the total charge and the second derivative of the emittance versus charge. The process is iterated until a certain stopping level is reached, in our case when the remaining charge in the phase space is the 80% of the starting charge value.

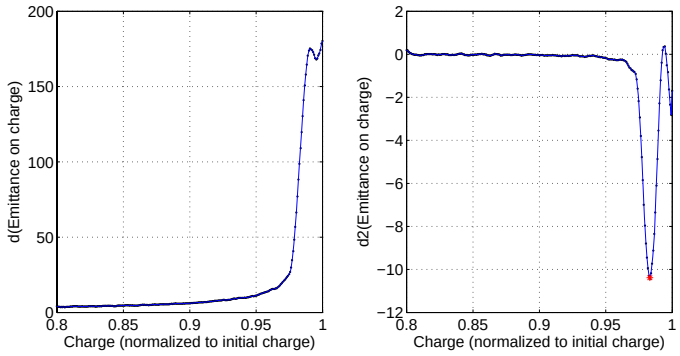

Figure 5: Example of a real signal measured. Left: first derivative of emittance versus charge. Right: second derivative of emittance versus charge

In Fig. 5 are shown the first and second derivatives of emittance versus charge. It can be appreciate that the strong peak in the right plot happens when there is a change in the slope on the left plot. Starting from this point and moving toward lower charge the slope of the first derivative tends to a small constant value. This regime is what is expected in the case of uniform beam phase space distribution. On the other end when the slope is very high, i.e. there is a strong variation of the emittance with the charge, it

seems reasonable associate this behavior to the beam halo or to the background. We use the peak in the second order derivative as an intrinsic marker of the separation between the beam and some halo or background noise. Starting from this point, assumed as 100% of the real beam charge, it is possible to calculate the value of the emittance versus charge at every level of cut.

Even if the larger number of the derivative curves look like Fig. 5 some distribution of the beam phase space produced different behavior. In particular double peak situation was sometime observed such as in Fig. 6.

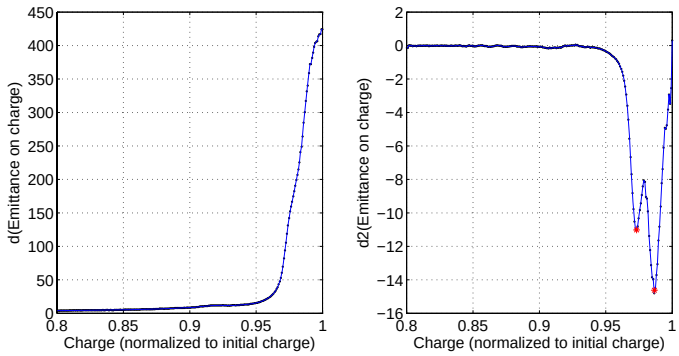

Figure 6: Example of a real signal with double peaks structure. Left: first derivative of emittance vs charge. Right: second derivative of emittance vs charge

This situation can be related to a less degree of connection in the phase space topology. It is well illustrated in Fig. 7.

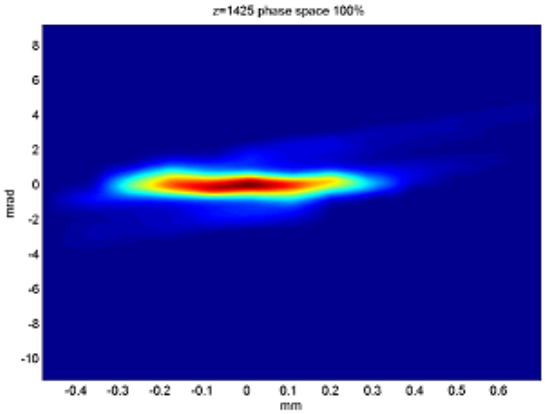

Figure 7: Phase space with typical cross shape

Here a bifurcation of the phase space is clearly visible. This condition is expected also from the simulation because different longitudinal slice of the beam, having differ-

ent charge and energy, after the solenoid, oscillate with different frequencies. On this consideration is based another algorithm for the phase space analysis [5] using a genetic algorithm. In the situation of double peak the 100% equivalent charge is assigned to the value of the peak with highest charge.

3 Monte Carlo simulations

3.1 General consideration

The phenomenological evidence of a sharp peak in the second derivative, always visible in all of our data, must be associated with something intrinsic in the signal. We start with an uniform round beam, over a noisy background gaussian distributed, with zero baseline and with sigma of 10% of the signal. The percentage number of the particles inside the beam area is 0.925

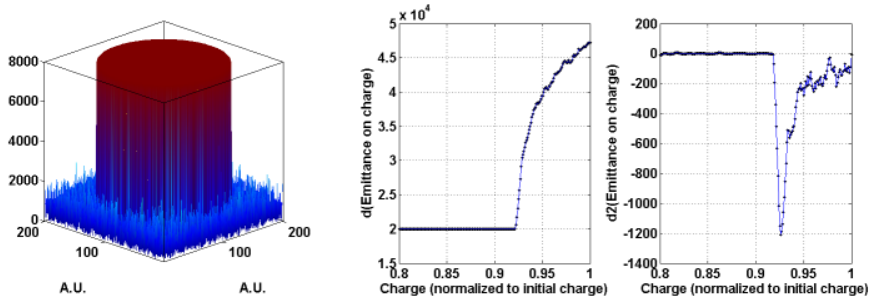

Figure 8: Left: signal model. Right: first and second derivative of emittance vs charge

In Fig. 8 is shown on the left the model used for the computation and the first and second order derivatives of emittance versus charge on the right. The position of the peak in the second order derivative is exactly at 92.5% of the total charge. This is a first indication that this peak is related with a suddenly change in the intensity distribution.

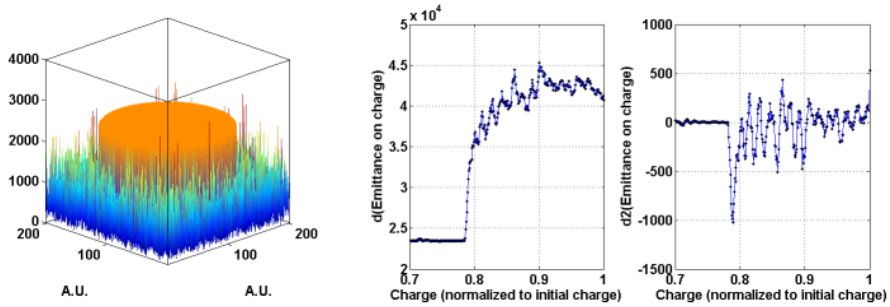

Figure 9: The same case of Fig. 8 but with lower SNR ratio

The difference of Fig. 9 respect to Fig. 8 is the amplitude of the signal, now decreased for a factor 3.33 respect to the former case. Also in this condition, even if the noise is much greater, the peak in the second derivative falls exactly at 78.76 % where it was expected. The SNR seems not to affect so much the presence of the peak.

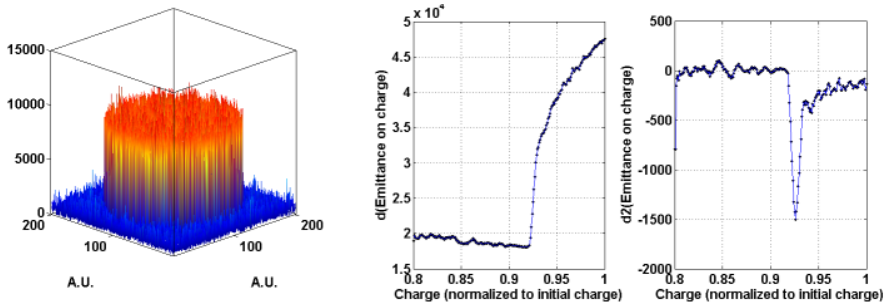

Figure 10: Some noise added also in the signal area

If we consider now to have some noise (gaussian distributed with σ=10% of the amplitude of the signal) also in the beam area we can appreciate from Fig. 10 that this noise affect only the region of the distribution of the derivative on the left of the peak.

The cylindrical uniform model is a too crude approximation of a real phase space beam. In particular the edge is maybe too sharp. A complete difference model is to consider a cone instead of a cylinder. In Fig. 11 is shown the case with a cone, collecting the 89.7% of the total charge and with a vertex 10 times higher than the background fluctuation. Also in this case is still present a small sharp transition between the cone and the noisy background.

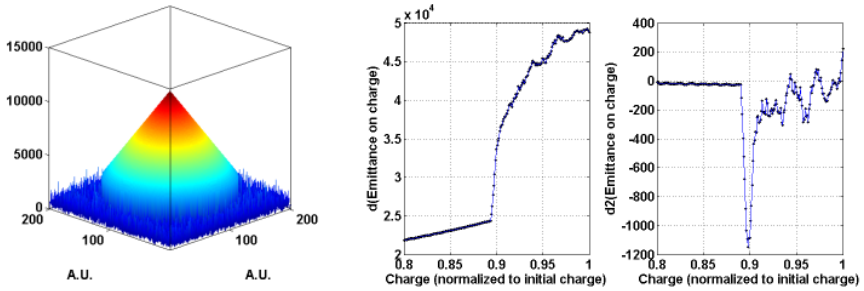

Figure 11: Cone model

If we cut it away, leaving the side to the cone to be completely drowned by the noise the expected transition a 78.4% disappears (see Fig. 12).

The same is also true for a Gaussian distribution, with no baseline that falls smoothly toward the noisy background (see Fig. 13)

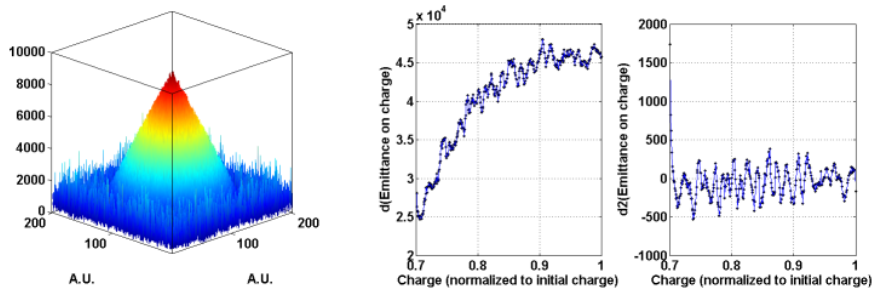

Figure 12: Cone model with no step between signal and noise

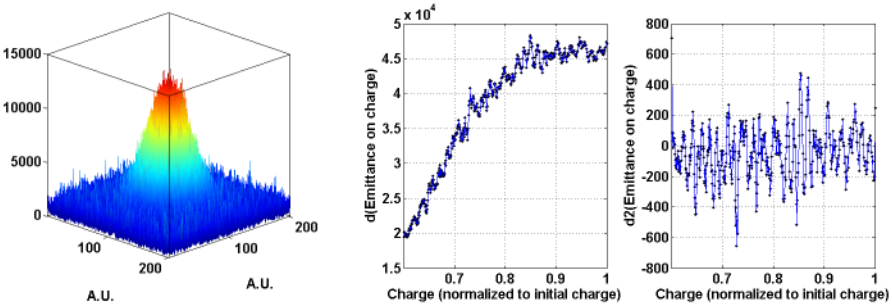

Figure 13: Gaussian model

But again if we sum a small sharp cylindrical baseline below to the gaussian we can obtain the peak in the second order derivative in the right position (see Fig. 14)

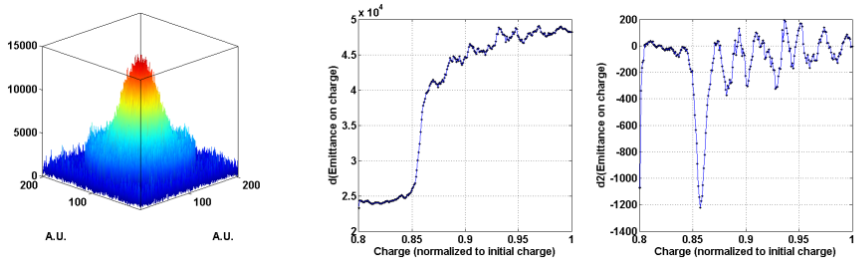

Figure 14: Gaussian model with sharp baseline under it

From these plot appears that the key factor is not the signal to noise ratio (or nor only) but a key role is played by the rise time of the signal from the noise.

3.2 Signal models

Studying the shape of the phase space signal that comes from the experimental data, a nice model seems to be a rotation paraboloid of the equation

$$z = a - a(\frac{x^2}{b^2} + \frac{y^2}{c^2})^d \tag{6}$$

where *a* is the scale factor, *b*,*c* constants and *d* is the order of the curve. For sake of simplicity, and because is not relevant for our discussion we assume here *b*=*c*, while in a real case they are, of course, different. Fractional value of *d* don't give a clear marker, neither reproduce the experimental behavior of the derivatives curves, while $d \geq 1$ not only produces a sharp peak in the second order derivative but also approximate very well the experimental data. The case of *d*=0.5 is shown in Fig. 15 where not appreciable difference can be found respect to the Fig. 12.

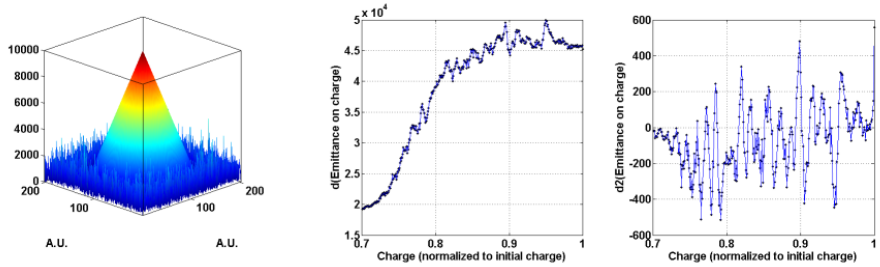

Figure 15: Parameter used:*a*=10000;*b*=40;*d*=0.5;background σ=1000

Already using *d*=2 produce the apparency of the peak in the plot of the derivative (Fig. 16).

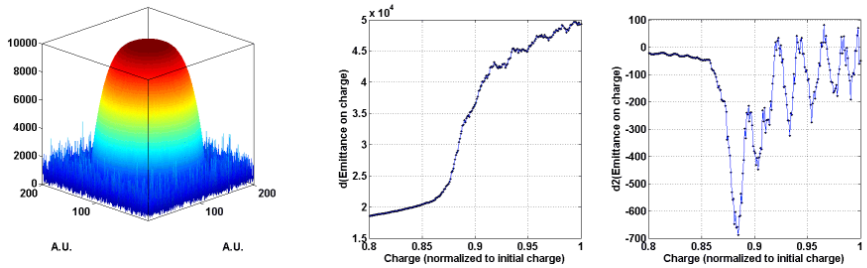

Figure 16: Parameter used:*a*=10000;*b*=40;*d*=2;background σ=1000

Even better if we increase the d parameter to the value d=20 as it is shown in Fig. 17. From these plot it is so clear that the key factor for the genesis of the peak is the speed of the signal increment over the noisy background.

We compared an experimental situation with our model. In particular the measurements of 26/10/2006 with solenoid field 127A in the vertical plane. The position is z=1425 mm from the cathode.

In Fig. 18 is possible to appreciate the good agreement between the model and the experimental data. The absolute value of the scale is, off course, meaningless.

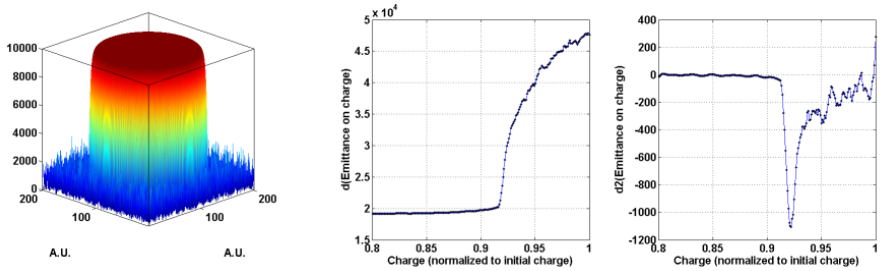

Figure 17: Parameter used:a=10000;b=40;d=20;background σ=1000

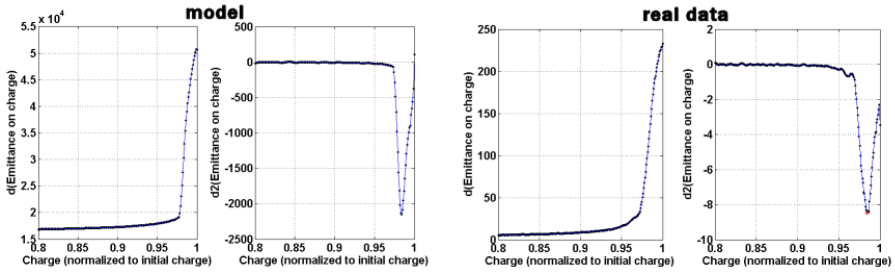

Figure 18: Parameter used:a=25000;b=c=79;d=10

4 Results comparison with other algorithms

In Figura 19 we compare results with the others two algorithms ([2], [5]) developed for this data analysis with this one.

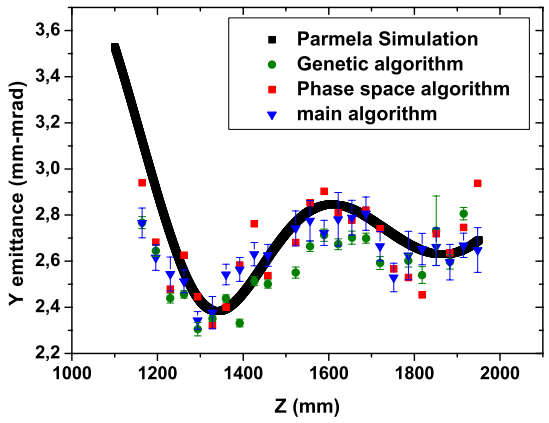

Figure 19: Comparison with other algorithms

We have chosen for this comparison one of the most significant measurement, giv-

ing the double minimum emittance oscillation, realized on Nov 26th 2006. The small amplitude of this oscillation is an excellent candidate to be used for a comparison between different methods to check if every method is able to resolve it. The cutting level for the phase space algorithm and for the genetic is 95%. The very good agreement is another confirmation that the algorithm [2] is well tuned for this application. Also in this way we give the quantitative estimation of the cut of the algorithm [2] that we wanted to find.

5 Conclusion

We developed an algorithm for phase space image data analysis. This tool, assuming a phenomenological evidence in the data distribution and relating it to a marker of the separation between signal and noise, is able to retrieve the emittance value and the Twiss parameters directly from phase space. It also allowed to quantify the cut level in the algorithm [2] used for data analysis.

References

[1] L. Catani *et al*,"Design and characterization of a movable emittance meter for low-energy electron beams", Review of Scientific Instruments 77, 93301 (2006).

[2] D. Filippetto, "A robust algorithm for beam emittance and trace space evolution reconstruction" Sparc Note SPARC/EBD-07/002 (2007).

[3] S.G. Anderson, J. B. Rosenzweig, G. P. Le Sage, J. K. Crane, Phys. Rev. ST Accel Beams,5,14201,2002

[4] Claude Lejeune and Jean Aubert, Adv. Electron. Electron Phys Suppl. 13A,159, 1980

[5] A.Bacci, "A genetic code able to compute the emittance value of a real beam by Multiple Ellipse Slice Analysis of the transversal phase space image" Sparc Note SPARC/EBD-07/004 (2007).